

# Morphotropic Phase Boundary in Solution-Derived $(\text{Bi}_{0.5}\text{Na}_{0.5})_{1-x}\text{Ba}_x\text{TiO}_3$ Thin Films: Part II Functional Properties and Phase Stability

Armando Perez-Rivero,<sup>‡</sup> Jesus Ricote,<sup>‡</sup> Inigo Bretos,<sup>‡</sup> M. L. Calzada,<sup>‡</sup> Javier Pérez de la Cruz,<sup>§</sup> Jose R.A. Fernandes,<sup>§,¶</sup> and Ricardo Jiménez<sup>‡,†</sup>

<sup>‡</sup>Instituto de Ciencia de Materiales de Madrid, CSIC, Cantoblanco, Madrid 28049, Spain

<sup>§</sup>INESC TEC, Instituto de Engenharia de Sistemas e Computadores do Porto, Porto 4200-465, Portugal

<sup>¶</sup>Universidade de Trás-os-Montes e Alto Douro, Vila Real 5001-801, Portugal

The analysis of the functional properties (ferroelectric, dielectric, and piezoelectric) of chemical solution deposited thin films of the lead-free  $(\text{Bi}_{0.5}\text{Na}_{0.5})_{1-x}\text{Ba}_x\text{TiO}_3$  (BNBT) solid solution prepared from solution precursors with and without  $\text{Na}^+$  and  $\text{Bi}^{3+}$  excesses has been performed in this work. At room temperature a nonergodic relaxor ferroelectric state has been found. The switched polarization of the films is not stable at room temperature, poor remnant polarization, associated with an enhancement of the induced domains randomization produced by the films constraints. The depolarization temperature for the switched polarization allowed us to build up a tentative phase diagram for these BNBT films. Both the better functional properties and the agreement of the depolarization temperature with the freezing temperature of the relaxor Volger–Fulcher behavior permit to locate the center of the morphotropic phase boundary region close to  $x = 0.055$  in the stoichiometric films and  $x = 0.10$  for the films with  $\text{Na}^+$  and  $\text{Bi}^{3+}$  excesses. Based on these results, the possible applications of these films are discussed.

## I. Introduction

THE use of piezoelectric materials has considerably increased in the last decades, mainly as sensors and transducers elements in electromechanical devices. Ferroelectric ceramics have been considered especially suitable for this type of applications due to their high piezoelectric coefficients.<sup>1,2</sup> Nowadays, the majority of these devices used materials based on the  $\text{PbZrO}_3$ – $\text{PbTiO}_3$  (PZT) solid solution. This presents enhanced piezoelectric coefficients for compositions near to the center of the morphotropic phase boundary region (cMPB), phase composition where two structural polymorphs present almost the same free energy. These structural instabilities lead to optimized piezoelectric and dielectric properties.<sup>3</sup> However, the strict environmental regulations that are being enforced worldwide have prompted the search for lead-free compositions with piezoelectric properties capable to replace the compositions with lead.<sup>4</sup> Among others, the solid solution of  $(\text{Bi}_{0.5}\text{Na}_{0.5})_{1-x}\text{Ba}_x\text{TiO}_3$  (BNBT) is a promising candidate. This presents a MPB region for compositions centered at  $x \approx 0.06$ .<sup>5</sup> Bulk ceramics with compositions near the cMPB showed enhanced piezoelectric and dielectric properties similar to those of the PZT system.<sup>6</sup> The  $d_{33}$  piezoelectric coefficient for cMPB BNBT bulk materials

is about 125 pC/N. Recently, Sapper *et al.*<sup>7</sup> found that the enhancement of the properties in the cMPB is not so much related to structural instabilities, but to the possibility of texturing of the domain configuration in the dominant rhombohedral or tetragonal phase. This can be the reason that no so large values of the functional properties in the cMPB BNBT compositions are observed compared with the strong optimization found out in cMPB PZT. The phase diagram of the BNBT solid solutions under the high electric fields has been recently reported for bulk ceramics. It is quite complex, thus indicating new field-induced MPB's for BNBT compositions with  $x = 0.08$  and  $0.07$ .<sup>8</sup> Moreover, it seems that for  $x = 0.08$ , the poling field eliminates the phase coexistence at the MPB producing a single-phase material, where no so large values of the piezoelectric coefficients are obtained.

The preparation of these materials in thin film form, preserving piezoelectric behavior, is essential for integration of functional materials in microelectronic devices.<sup>9,10</sup> This interest has given rise to the publication of several works on the preparation of BNBT thin films.<sup>11–14</sup> As long as functional properties depend on the crystal structure, the knowledge of the phase diagram of BNBT thin films is of major importance. Several phase diagrams have been reported for bulk materials.<sup>15–18</sup> It has been reported in,<sup>19</sup> that in the MPB region, with increasing temperature, a ferroelectric-relaxor (FE-RE) transition occurs and that the ferroelectric-antiferroelectric transition<sup>5</sup> is a result of the induced electric field on the FE-RE transition. The relaxor nature of the  $\text{Na}_{0.5}\text{Bi}_{0.5}\text{TiO}_3$  phase was also proposed by Dorcet *et al.*<sup>20</sup> For better understanding of the implications of relaxor ferroelectric state, the reading of the article of Bokov and Ye<sup>21</sup> is recommended. Therefore, if the FE state of BNBT at the MPB comes from the growing of FE domains under an electric field, in a phase presenting a nonergodic relaxor state at room temperature,<sup>21</sup> a strong effect of the grain size on the ferroelectric state stability should be observed.<sup>22</sup>

The structural and compositional study carried out in the Part I of this work<sup>23</sup> concludes that no displacement of the MPB occurs at room temperature in the stoichiometric BNBT films ( $x$  values between 0.055 and 0.08). However, the MPB of the films with  $\text{Bi}^{3+}$  and  $\text{Na}^+$  excesses appears close to nominal values of  $x \approx 0.10$ , suggesting that the  $\text{Bi}^{3+}$  and  $\text{Na}^+$  excesses remain in the bulk film, total or partially incorporated to the A-sites of the perovskite. This needs of the transfer of Ti ions from  $\text{BaTiO}_3$  to  $(\text{Bi}_{0.5}\text{Na}_{0.5})\text{TiO}_3$  in the BNBT solid solution, resulting in an “apparent” movement of the MPB, in free BaO and in the formation of secondary phases.

The stability of the ferroelectric polarization with time and temperature is essential to determine the applications of these films in devices. Strong remnant properties and a wide temperature stability range are essential for piezoelectricity-based

D. Damjanovic—contributing editor

Manuscript No. 33418. Received June 24, 2013; approved November 9, 2013.

<sup>†</sup>Author to whom correspondence should be addressed. e-mail: rijim@icmm.csic.es

applications (sensors and high accuracy actuation devices). Moreover, bulk materials of this solid solution with values of  $x =$  around 0.10 have been proposed as active elements for pyroelectric energy harvesting and electrocaloric effect-based applications, where large remnant properties are not required but a large enough change in the properties as a function of the applied electric field.<sup>24–26</sup>

This work studies the functional properties (ferroelectric, dielectric, and piezoelectric) of solution-derived BNBT thin films on Pt-coated Si substrates as function of temperature, paying attention to the effect of time on the induced polarization. Films with nominal compositions in a wide range of  $x$  values, between 0.035 and 0.15, with/without  $\text{Bi}^{3+}$  and  $\text{Na}^+$  excesses are analyzed.

The dielectric and ferroelectric properties are characterized as a function of temperature, to establish the stability of the ferroelectric properties and possible phase transitions. The aim is to correlate these results with the reported phase diagrams for bulk materials and the crystal structure, microstructure and heterostructure of these thin films reported in the Part I of this work.<sup>23</sup> Application of these films in devices is discussed based on the properties here shown.

## II. Experimental Procedure

$(\text{Bi}_{0.5}\text{Na}_{0.5})_{1-x}\text{Ba}_x\text{TiO}_3$  films were prepared by chemical solution deposition, using a solution process previously described.<sup>23,27</sup> Two sets of films were prepared; stoichiometric ones with  $x$  values of 0.035 (BNBT3.5), 0.055 (BNBT5.5), 0.080 (BNBT8.0), 0.100 (BNBT10.0) and with 10 mol% of  $\text{Bi}^{3+}$  and  $\text{Na}^+$  excesses, with nominal  $x$  values of 0.055 (BNBT5.5xs), 0.100 (BNBT10.0xs) and 0.150 (BNBT15.0xs).

For the electrical characterization of discrete planar capacitors, top electrodes of Pt/Au with 200  $\mu\text{m}$  in diameter were deposited on the film surfaces by D.C. sputtering.

The macroscopic piezoelectric hysteresis loops were carried out by using a fiber-optic, double-beam incidence Mach-Zehnder interferometer, as reported elsewhere.<sup>28</sup> The measurements were performed using an AC driving voltage of 5 V at 7.5 kHz with a maximum electric field of 220  $\text{kV}/\text{cm}$ .

Ferroelectric hysteresis loops were obtained by means of an in-house made system which is equipped with a virtual ground circuit, an oscilloscope (TDS520; Tektronix, Inc., Beaverton, OR) and a pulse generator (8116A; HP GmbH, Boeblingen, Germany).<sup>29</sup> To obtain pure ferroelectric switching loops, the nonferroelectric switching contributions to the loops were compensated by software.<sup>30</sup> Note that the remnant polarization obtained from “conventional” compensated hysteresis loops corresponds to the maximum remnant polarization ( $P_{\text{rmax}}$ ) because the sample keeps the zero field just for a small fraction of time.

Hysteresis remnant polarization loops<sup>31</sup> were measured in the commercial RADIANT Precision Premier II equipment. This permits to extract the remnant loop after 1 s of relaxation. The comparison of  $P_{\text{rmax}}$  from the corrected and remnant loops indicates the temporal stability of the ferroelectric polarization. The loops were traced at 1 KHz (1 ms) with a maximum applied voltage of 20 V.

The temperature dependence of the dielectric permittivity and losses were measured with a Precision LCR meter (HP 4284) at several frequencies between 100 Hz and 1 MHz, from room temperature (RT) to 350°C, with heating and cooling rates of 1.5°C/min.

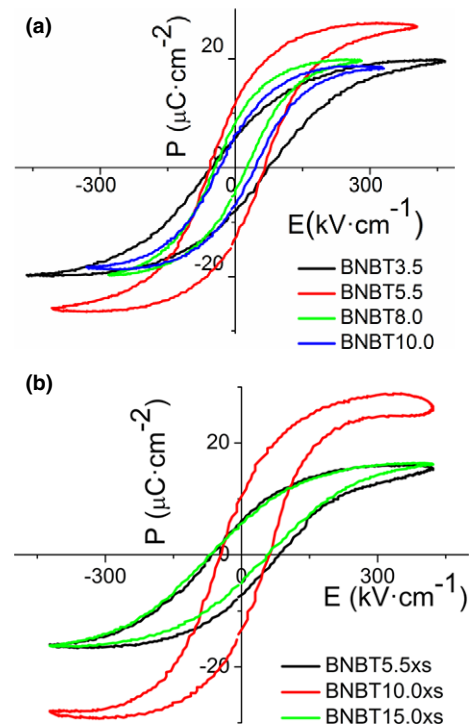
The evolution of the ferroelectric polarization with the temperature was measured with the in-house ferroelectric loops system keeping the sample in a controlled temperature measurement jig. The measurements were carried out from RT to 300°C, in 25°C steps and with a frequency of 10 kHz, to minimize conductivity contributions in the overall temperature range. The maximum field applied is always more than 2.5 times the coercive field ( $E_c$ ), to assure the complete poling of the samples.

## II. Results

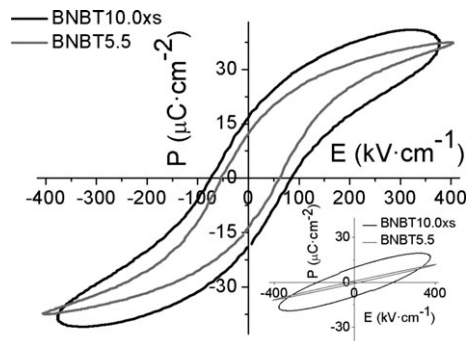
### (1) Ferroelectric Loops

Figure 1(a) shows the room temperature compensated ferroelectric loops of the films without excesses of  $\text{Bi}^{3+}$  and  $\text{Na}^+$ , where the nonswitching contribution was eliminated. The BNBT5.5 sample has the highest value of remnant polarization, with  $P_r = 12.3 \mu\text{C}/\text{cm}^2$ , whereas films BNBT3.5, BNBT8.0 and BNBT10.0 have lower values,  $P_r = 6.7 \mu\text{C}/\text{cm}^2$ ,  $P_r = 6.3 \mu\text{C}/\text{cm}^2$ , and  $P_r = 6.4 \mu\text{C}/\text{cm}^2$ , respectively. These loops for the samples with a 10% excess of  $\text{Bi}^{3+}$  and  $\text{Na}^+$ , Fig. 1(b), indicate that the maximum value of remnant polarization,  $P_r = 11.9 \mu\text{C}/\text{cm}^2$ , is obtained in the BNBT10.0xs film, whereas the BNBT5.5xs and BNBT15.0xs samples show lower values,  $P_r = 6.6 \mu\text{C}/\text{cm}^2$  and  $P_r = 5.4 \mu\text{C}/\text{cm}^2$ , respectively. From the point of view of the ferroelectric polarization, the films with enhanced properties are those with compositions close to the cMPB,  $x$  values of  $x = 0.055$  and 0.100 for the BNBT and BNBTxs films, respectively. These results are in agreement with those about the crystal structure reported in.<sup>23</sup> It is interesting to note that the electric behavior of the films with and without these excesses is different. In the case of the BNBTxs films, the nonswitching contributions to the FE loop are more important; due to the effect of a larger conductivity and the onset of the leakage currents. In Fig. 2, the experimental loops of the BNBT5.5 and BNBT10.0xs films are plotted. The BNBT10.0xs film presents rounded ferroelectric hysteresis loops, indicating a strong contribution of conductivity. The nonswitching charge for this sample is 20 times larger at a zero external field (conductivity contribution) than that of the BNBT5.5 thin film, inset of Fig. 2. This can be related with the differences in composition and microstructure and reported in.<sup>23</sup> Roughness and porosity are larger for the BNBTxs films than for the BNBT films and, in addition, the former develop nonhomogeneous compositional depth profiles.

A FE-RE transition has been proposed as responsible of the anomalies in the electric properties observed in this system at intermediate temperatures.<sup>19</sup> Thus, it is highly impor-



**Fig. 1.** Compensated hysteresis loops measured at 1 kHz, as function of the  $\text{BaTiO}_3$  content. (a) BNBT thin films. (b) BNBTxs thin films.



**Fig. 2.** (a) Experimental polarization hysteresis loops for the films BNBT5.5 measured at 1 kHz. (b) Nonswitching contribution to the polarization loops.

tant to know how polarization relaxes with time. For RE materials, the difference between the  $P_{\text{rmax}}$  (unrelaxed) obtained from the “conventional” hysteresis loops and the polarization from the remnant loop (relaxed at 1 s) is very large. On the contrary, for FE thin film the difference between  $P_{\text{rmax}}$  and the remnant loop is almost zero. Figure 3(a) shows the remnant ferroelectric hysteresis loops for the BNBT thin films. A strong difference between the half-loops traced with positive voltage in comparison with the half-loops traced with negative voltage is observed. This effect is larger for the BNBT3.5, 8.0, and 10.0 than for the BNBT5.5 film where it is almost zero. This nonsymmetry of the remnant polarization with respect to the external field is related to imprint effects, mainly due to self-polarization effects that cannot be solved by electrical cycling. On the contrary, the symmetry of the remnant loop of the BNBT5.5 sample suggests a more efficient switching, which is able to change the initial FE polarization situation of the film. The remnant polarization values obtained from the hysteresis loops of Fig. 3(a) are lower than the  $P_{\text{rmax}}$  values obtained from the loops of Fig. 1. The BNBT3.5 and BNBT8.0 samples loss around 70% of their  $P_{\text{rmax}}$  after 1 s of relaxation.

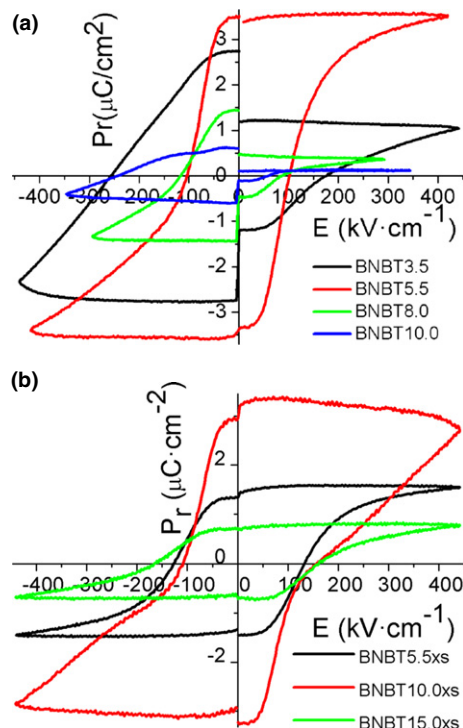


**Fig. 3.** Remnant hysteresis loops. (a) BNBT films. (b) BNBTxs films.

This is even worse for the BNBT10.0 film that loss around 95% of its initial polarization. The situation is slightly different in the films with  $\text{Bi}^{3+}$  and  $\text{Na}^{+}$  excesses, Fig. 3(b). The loops of the BNBTxs films are symmetric, indicating no imprint, but the relaxation of the polarization is also strong; 80%, 75%, and 86%, for the BNBT5.5xs, BNBT10.5xs, and BNBT15.0xs films, respectively. Based on these results, it can be inferred that the stability with time of the FE polarization is low in these samples, supporting the idea of an induced FE polarization from a RE state at room temperature, in the films of this solid solution. This instability of the polarization in thin films of relaxor-based solid solutions has been previously observed in  $\text{Pb}(\text{Mg}_{1/3}\text{Nb}_{2/3})\text{O}_3\text{-PbTiO}_3$  (PMNT) materials for compositions in the MPB region and related to the grain size.<sup>32</sup> On reducing the grain size, a change in the domain configuration is produced that is a consequence of the slowdown of the transition from the relaxor to the ferroelectric state that hinders the ferroelectric switching. Moreover, when this PMNT material is prepared as polycrystalline thin film form, the loops are strongly slanted and a strong relaxation of the polarization is obtained after 1 s.<sup>33,34</sup>

## (2) Evolution of the Ferroelectric Polarization with the Temperature

The behavior of the ferroelectric polarization as a function of temperature under switching conditions was studied for each of the films by measuring the hysteresis loops on increasing temperature. Figure 4 presents the compensated loops as a function of temperature for the BNBT10.0 sample. A reduction of both the  $P_{\text{rmax}}$  and the saturation polarization ( $P_s$ ) is observed. Moreover, the coercive field ( $E_c$ ) decreases as the temperature increases. This is the general behavior for all the films of this work. It is important to point up that in any case, AFE-like or “pinched” loops are obtained. The evolution of  $P_{\text{rmax}}$  and  $E_c$  with temperature for the BNBT and BNBTxs films is plotted in Fig. 5. The  $P_{\text{rmax}}$  presents a continuous reduction on increasing temperature with a kink, where the drop of the  $P_{\text{rmax}}$  against the temperature is stronger. To determine the temperature of where this occurs, the pyroelectric coefficients ( $\gamma = dP/dT$ ) were calculated from the derivative of the interpolated  $P_{\text{rmax}}$  versus  $T$  curves (insets of Figs. 5 and 6). A minimum value of the pyroelectric coefficient is observed (depolarization) for all the films, at the temperature where the kink in the polarization evolution with temperature takes place [insets of Figs. 5(a)–(d)]. The temperature of these minima are 162°C, 137°C, 240°C, and 268°C for the BNBT3.5, BNBT5.5, BNBT8.0, and BNBT10.0 thin films, respectively. These temperatures for the BNBTxs samples [Figs. 6(a)–(c)] are 216°C, 137°C, and 244°C for the BNBT5.5xs, BNBT10.0xs, and BNBT15.5xs films, respectively. The evolution of the coercive field with

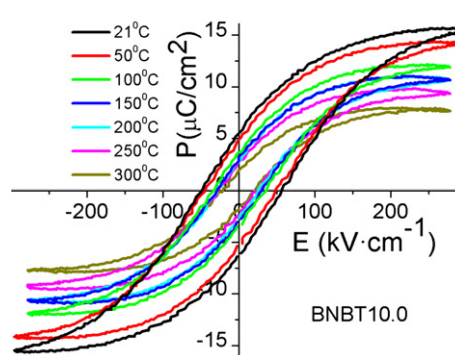


**Fig. 4.** Compensated ferroelectric polarization loops as function of increasing temperature for the BNBT10.0xs sample.

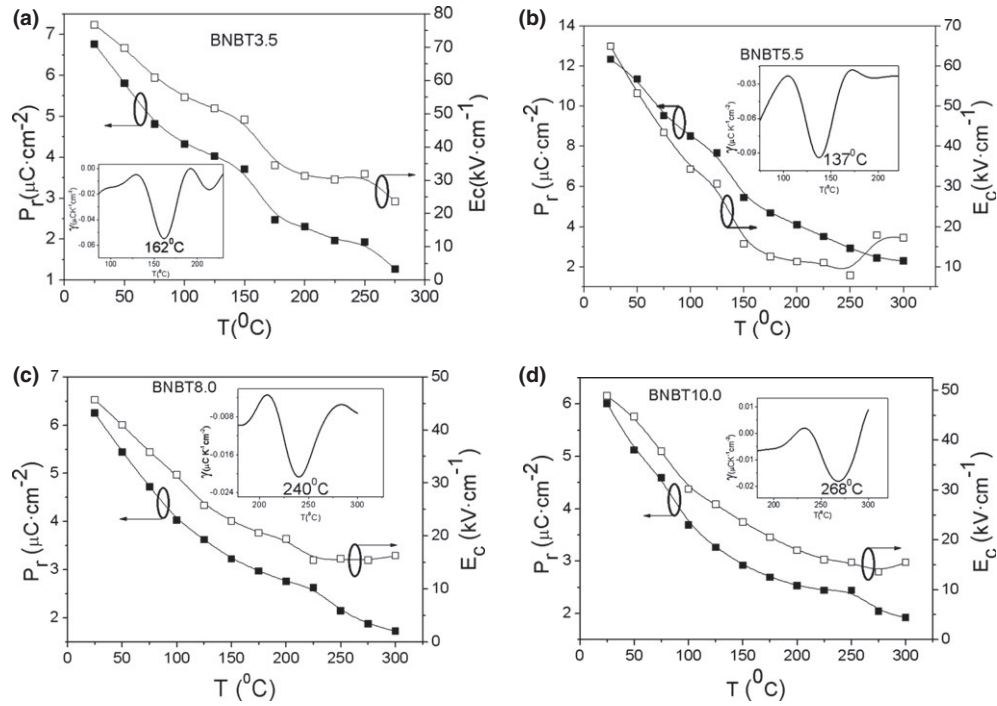


**Fig. 5.** Behavior of the ferroelectric properties with temperature in the BNBT films. Curves show the behavior of the maximum remnant polarization ( $P_{r\max}$ ) and coercive field ( $E_c$ ) with the temperature for (a) BNBT3.5, (b) BNBT5.5, (c) BNBT8.0, (d) BNBT10.0. Insets show the evolution of the pyroelectric coefficient as a function of the temperature.

temperature observed in Figs. 5 and 6 showed a similar evolution as that of  $P_{r\max}$ . This temperature can be identified as the depolarization temperature  $T_d$ .<sup>7</sup> On further increase in the temperature, the  $P_{r\max}$  slowly drops to zero, but the high conductivity contribution prevents the observation of the vanishing of the ferroelectric polarization.

### (3) Low Field Dielectric Behavior with the Temperature

The variation in both real and imaginary parts of the dielectric permittivity with temperature is shown in Fig. 7 for the BNBT5.5 and BNBT10.0xs samples, measured under a cooling run condition. The dielectric response of these films is similar, presenting as a main difference the values of the dielectric loss on increasing temperatures, due to large conductivity contributions in the BNBT10.0xs film. The dielectric constant of the BNBT5.5 film presents a broad maximum at 220°C without frequency shift on increasing the temperature [Fig. 7(a)]. For dielectric loss, a maximum at lower temperatures is observed that shifts to higher temperatures and larger values on increasing the temperature. This behavior resembles that of RE ferroelectrics. The Volger–Fulcher plot for the maxima of the dielectric loss and the fitting of these maximum values are shown in the inset of Fig. 7(a). A freezing temperature of the polar nanoregions (PNRs) of  $T_f = 135^\circ\text{C}$  is obtained, with an activation energy of 0.33 eV and a relaxation time of  $\tau_0 = 9.43 \times 10^{-6}$  s. This relaxation time is quite high, but notice that the calculation of this parameter has a large error due to the limited frequency window used in the measurements.

These dielectric results are consistent with a ferroelectric-to-relaxor transition in the BNBT thin films with compositions close to the cMPB. The existence of  $T_f$  indicates a state change from an ergodic to a nonergodic state, but, however, it does not give information about the possible appearance of a FE state with stable ferroelectric domains under electric field. The  $T_f$  value of  $\sim 135^\circ\text{C}$  matches well with the temperature of the minimum in the pyroelectric coefficient for this film,  $\sim 137^\circ\text{C}$ . This supports the idea that the observed kink in the evolution of  $P_{r\max}$  with temperature should be related

with a change from a nonergodic relaxor state, with field-induced FE domains, to an ergodic relaxor state.

The dielectric behavior as function of temperature for the BNBT10.0xs sample is presented in Fig. 7(b). The dielectric constant presents a broad maximum centered at  $241^\circ\text{C}$ . The evolution of the dielectric loss with temperature shows a maximum that shifts to higher temperatures on increasing the frequency. The large conductivity contribution to the losses makes difficult to extract the Volger–Fulcher behavior. Similar behaviors are also observed for the other BNBT and BNBTxs films. The variation in the dielectric permittivity with temperature of the BNBT3.5, BNBT8.0, and BNBT10.0 films also shows broad maxima at  $227^\circ\text{C}$ ,  $228^\circ\text{C}$ , and  $258^\circ\text{C}$ , respectively, with maxima of the dielectric losses clearly visible at 10 kHz for intermediate temperatures, but not observable at low frequencies due to conductivity. For the films containing  $\text{Bi}^{3+}$  and  $\text{Na}^+$  excesses, a strong conductivity is observed, obtaining broad maxima of the dielectric permittivity at  $240^\circ\text{C}$  and  $264^\circ\text{C}$  for the BNBT5.5xs and BNBT15.0xs films, respectively. A maximum in the dielectric losses at intermediate temperatures is only observed here for the BNBT10.0xs film. The similarities between the dielectric behavior of the BNBT5.5 and BNBT10.0xs samples allowed us to state that the minimum in the pyroelectric coefficient associated with the drop in  $P_{r\max}$  can be related to the nonergodic to ergodic transition in RE ferroelectric materials, at least for these two thin films.

### (4) Macroscopic Piezoelectric Properties

The macroscopic piezoelectric properties of the films of this work have been defined by the macroscopic effective piezoelectric coefficient,  $d_{33\text{eff}}$  versus electric field loops (Fig. 8). The BNBT5.5 and BNBT8.0 films present the largest response, with  $d_{33\text{eff}}$  values of  $\sim 18.75$  and  $19.21$  pm/V, whereas the BNBT3.5 film has a lower  $d_{33\text{eff}}$  value of  $\sim 10.93$  pm/V [see Fig. 8(a)]. The better piezoelectric properties of the BNBT5.5 and BNBT8.0 films are an indication of the proximity of the compositions of these films to the cMPB.<sup>23</sup> These results are in agreement with those obtained

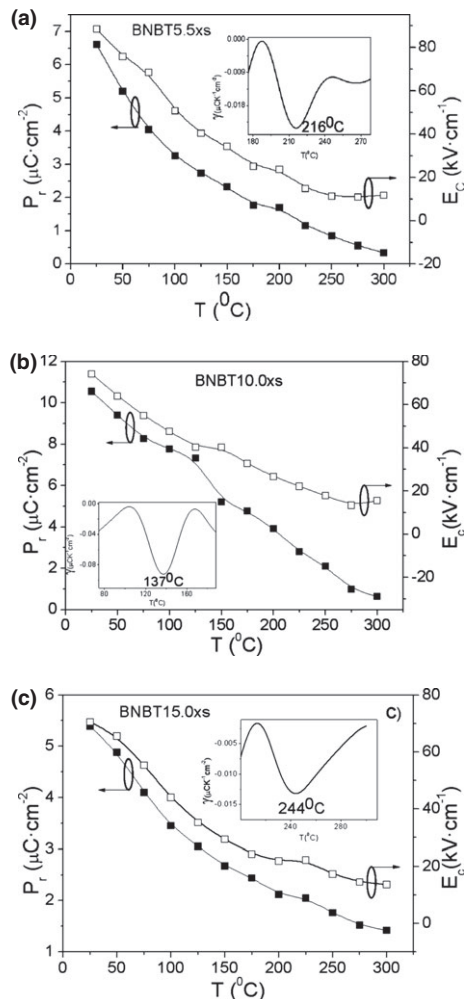


**Fig. 6.** Behavior of ferroelectric properties with temperature in the BNBTxs films. Curves show the behavior of the maximum remnant polarization ( $P_{rmax}$ ) and coercive field ( $E_c$ ) with the temperature for, (a) BNBT5.5xs, (b) BNBT10.0xs, (c) BNBT15.0xs. Insets show the evolution of the pyroelectric coefficient as a function of the temperature.

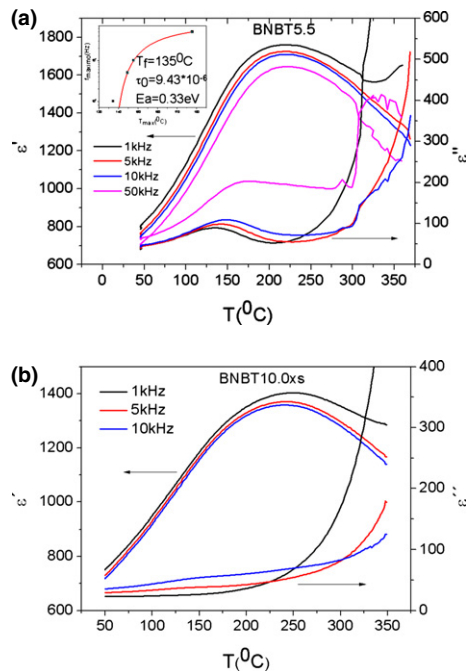
in the study of the  $P$ - $E$  loops and also with those previously reported for bulk ceramics.<sup>5,35</sup>

Figure 8(b) shows the  $d_{33eff}$  with the electric field loops for the samples prepared with excesses of  $Bi^{3+}$  and  $Na^+$ , in particular the BNBT5.5xs and BNBT10.0xs films. In both cases, the piezoelectric response is deformed, with anomalous  $d_{33eff}$  hysteresis loops at high fields. This behavior can be related with the large conductivity and leakage currents (current injection) of these samples that prevent a proper polarization at high fields.

#### IV. Discussion

It is difficult to compare the physical properties of thin films with those of bulk ceramics. Many of the characterization techniques used for bulk ceramic are not applicable to thin films. The constraints imposed by the heterostructure on the properties of the films can modify the state of the phases and so the comparison must be done with a special care. In addition, the results and derived conclusions found out in this study should be considered applicable to similar polycrystalline thin films.

The results here shown strongly support that these  $(Bi_{0.5}Na_{0.5})_{1-x}Ba_xTiO_3$  films are at room temperature in a nonergodic relaxor ferroelectric state. In this state and for temperatures below the  $T_f$ , ferroelectric domains can build



**Fig. 7.** Behavior of the real and imaginary relative dielectric permittivity for: (a) BNBT5.5, (b) BNBT10.0xs. Inset of (a) shows the Vogel-Fulcher curve.

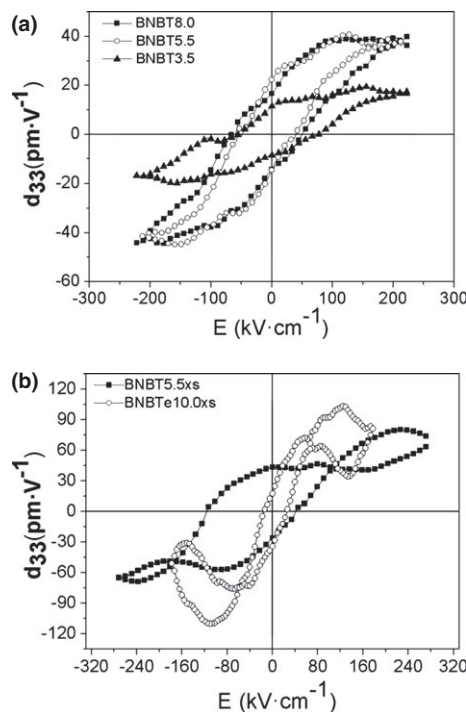


**Fig. 8.** Macroscopic piezoelectric hysteresis loops. (a) BNBT3.5, BNBT5.5 and BNBT8 and (b) BNBT5.5xs and BNBT10.0xs.

up under high electric fields and they can show some stability with time.<sup>19,21</sup> The reason behind this relaxor-like behavior of the  $(Bi_{0.5}Na_{0.5})_{1-x}Ba_xTiO_3$  solid solution can be related to the complex domain structure of the  $Na_{0.5}Bi_{0.5}TiO_3$  phase. Recent transmission electron microscopy studies (TEM)<sup>36</sup> demonstrate a strong tilting and chemical Bi/Na disorders in this phase, producing a shortening of the coherence length of the structure. Due to this relaxor character, the effect of the grain size on the stability of the FE domains should be strong, as previously demonstrated for the PMPT solid

solution.<sup>32–34</sup> Therefore, in thin films, with small grain sizes, the stabilization of a stable FE state with time, is not possible, even for compositions with small phase coexistence. These phenomena can be understood considering in these compounds a two-stage process for the FE to RE transition.<sup>37</sup> Large “texturized” FE switched domains suffer a randomization previous to the split in PNRs. This appears as a strong relaxation of the remnant polarization after a short time, here 1 s, Fig. 4. This randomization of the switched domains at room temperature prevents the measurement of the thermally stimulated currents in these samples, due to the fast depolarization.<sup>38</sup>

The enhancement of the switched domains randomization in thin films is produced by boundary conditions in thin films, such as small grain size, electrode/FE interfaces, and depth profile compositional/structural differences that lead to large extrinsic depolarization fields, in addition to that resulting from the internal random fields.

It has to be noted the agreement between  $T_d$  and  $T_f$  in the films with compositions close to the cMPB. Here, the free energies of the rhombohedral and tetragonal phases should almost be equal, so the easy conversion between both phases can produce an anticipation in the splitting of the polar domains to yield PNRs and give rise to the ergodic relaxor state. It is risky try to extract more information from the characterization of polycrystalline thin films, but the proximity of the  $T_d$  of the BNBT10 and BNBT15.5xs thin films to the  $T_m$  can be related to a larger stability of the tetragonal polar phase, for the compositions out of the cMPB, that keeps the nonergodic state to temperatures close to those of the maxima in the dielectric constant. The proximity of  $T_d$  ( $\approx T_f$ ) to  $T_m$  produces a kind of FE to paraelectric (PE) diffuse phase transition in our experimental conditions.

Our results indicate that the BNBT5.5 and BNBT10.0xs films have the best properties, as expected for compositions close to the cMPB. A tentative phase diagram can be proposed for these  $(\text{Bi}_{0.5}\text{Na}_{0.5})_{1-x}\text{Ba}_x\text{TiO}_3$  films, taking into account the results here obtained for the depolarization temperatures ( $T_d$ ) and main dielectric anomalies ( $T_m$ ), those results shown in the Part I of this study<sup>23</sup> and the phase diagram reported by Takenaka *et al.*<sup>5</sup> for bulk ceramics as shown in (Fig. 9). The films with the stoichiometric nominal compositions, the BNBT films, present a phase diagram

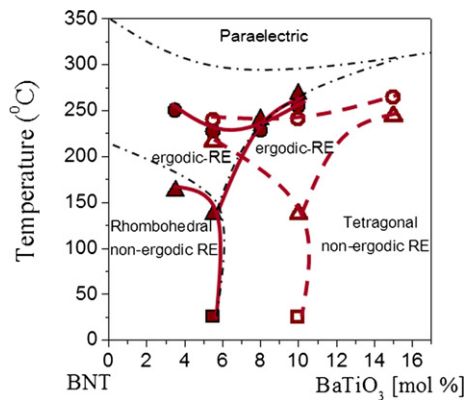


**Fig. 9.** Tentative phase diagram of the  $(\text{Bi}_{0.5}\text{Na}_{0.5})_{1-x}\text{Ba}_x\text{TiO}_3$  thin films of this work. The open and closed triangles indicate the depolarization temperatures for the BNBT and BNBTxs films, respectively. The closed and open circles indicate the temperature at the maximum of the broad dielectric anomaly, for the BNBT and BNBTxs films, respectively. The closed and open squares are obtained from the structural study in the part I.<sup>23</sup> Lines are a guide for the eye. The center of the morphotropic phased region (cMPB) is located approximately close to the minimum in the depolarization temperature. The dashed dot lines correspond to the phase diagram reported in Ref. [5].

similar to that of bulk ceramics (closed symbols in Fig. 9), with the cMPB in the vicinity of  $x \sim 0.055$  but the relaxor-to-paraelectric transition line is observed at lower temperature ( $50^\circ\text{C} - 70^\circ\text{C}$  lower) if compared with the Takenaka phase diagram (dash dot line in Fig. 9). At low  $\text{BaTiO}_3$  contents, a nonergodic relaxor state with a major rhombohedral polar phase is found. Higher amounts of  $\text{BaTiO}_3$  lead to a nonergodic relaxor with the tetragonal phase as the major one. On increasing the temperature the nonergodic relaxor transforms into an ergodic relaxor, possibly with only tetragonal PNRs. For a further increasing of the temperature, the films are the most part in a paraelectric cubic phase. In comparison with the Takenaka phase diagram, the nature of the phases is different. The supposed AFE phase is found to be an ergodic relaxor and the FE phases are nonergodic relaxors, where polar domains can be stabilized under an electric field. In the case of the BNBTxs films, containing  $\text{Bi}^{3+}$  and  $\text{Na}^+$  excesses (open symbols in Fig. 9), a displacement of the cMPB position to higher concentrations of  $\text{BaTiO}_3$  is observed, but qualitatively the general behavior of these films in the phase diagram is the same as that of the BNBT ones. Apart from the displacement of the MPB region toward larger nominal amounts of  $\text{BaTiO}_3$ , the effect of the  $\text{Bi}^{3+}$  and  $\text{Na}^+$  excesses is to increase the conductivity and leakages in the electric response. The origin of this enhanced conductivity should be related to the fact that not all of the excesses of these elements are lost by volatilization, some of them seem to incorporate to the crystal structure (see results of Part I,<sup>23</sup>), other remain in the bulk film (grain boundaries, second phases) or contribute to the formation of thick interfacial regions with the bottom electrode. In addition, the BNBTxs films also show a larger porosity and roughness than the BNBT films.<sup>23</sup>

About the possible applications of the  $(\text{Bi}_{0.5}\text{Na}_{0.5})_{1-x}\text{Ba}_x\text{TiO}_3$  thin films, the films prepared from stoichiometric solutions present better functional properties than those where the traditional excesses of the volatiles elements for processing thin films are used. However, the stability of the ferroelectric remnant polarization with time is not proved, so these films should not be used in applications requiring a large remanence of the ferro-piezoelectric properties. The loss of the switched polarization with time does not follow the same mechanism as that of relaxors at temperatures over  $T_d$  or  $T_f$ . Therefore, the large strain for high fields required for actuation is not assured. On the contrary, the polarization behavior of these samples seems to be of interest for thermoelectricity-related applications under electrical field.<sup>24–26</sup>

## V. Conclusions

1. The preparation of polycrystalline thin films of  $(\text{Bi}_{0.5}\text{Na}_{0.5})_{1-x}\text{Ba}_x\text{TiO}_3$  compositions produce phases that present at room temperature a nonergodic relaxor state where large FE domains can be induced under an electric field, but showing a poor remnant polarization.
2. The poor remnant properties can be related to an enhanced randomization of the switched domains produced by the small grain size and constrictions imposed by the heterostructure of the thin films.
3. The cMPB is close to  $x$  values of 0.055 for the films prepared from stoichiometric solutions and close to  $x \sim 0.100$  for the films with  $\text{Na}^+$ ,  $\text{Bi}^{3+}$  excesses (10%). However, the phase diagrams are qualitatively the same for the films with or without  $\text{Na}^+$ ,  $\text{Bi}^{3+}$  excesses.
4. At intermediate temperatures, a depolarization kink is found in the  $P_{\text{rmax}}$  that can be correlated with the Volger–Fulcher freezing temperature for the compositions in the near vicinity of the cMPB, where a FE nonergodic state change to an ergodic relaxor one can be demonstrated.

5. The  $\text{Bi}^{3+}$  and  $\text{Na}^{+}$  excesses (10%) in these films result in an “apparent” shift in the MPB region associated with structural changes produced by the incorporation of part of these excesses in the crystal phases, but also some of these excesses remain in the film leading to inhomogeneous film profiles responsible of the enhanced conductivity and leakage currents of these samples.

### Acknowledgments

This work was financed by Spanish Projects MAT2010-15365 and bilateral Portuguese-Spanish Project CRUP E14/11. A. Perez-Rivero acknowledges the support of the FPI program. I. Bretos acknowledges the support of the “Juan de la Cierva” Spanish program.

### References

- <sup>1</sup>D. L. Polla and L. F. Francis, “Processing and Characterization of Piezoelectric Materials and Integration into Microelectromechanical Systems,” *Annu. Rev. Mater. Sci.*, **28**, 563–97 (1998).
- <sup>2</sup>N. Setter, D. Damjanovic, L. Eng, G. Fox, S. Gevorgian, S. Hong, A. Kingon, H. Kohlstedt, N. Y. Park, G. B. Stephenson, I. Stolichnov, A. K. Taganov, D. V. Taylor, T. Yamada, and S. Streiffner, “Ferroelectric Thin Films: Review of Materials, Properties, and Applications,” *J. Appl. Phys.*, **100**, 051606, 46 pp (2006).
- <sup>3</sup>R. Guo, L. E. Cross, S. E. Park, B. Noheda, D. E. Cox, and G. Shirane, “Origin of the High Piezoelectric Response in  $\text{PbZr}_{1-x}\text{Ti}_x\text{O}_3$ ,” *Phys. Rev. Lett.*, **84**, 5423–6 (2000).
- <sup>4</sup>J. Rödel, W. Jo, K. T. P. Seifert, E. M. Anton, T. Granzow, and D. Damjanovic, “Perspective on the Development of Lead-Free Piezoceramics,” *J. Am. Ceram. Soc.*, **92**, 1153–77 (2009).
- <sup>5</sup>T. Takenaka, K. Maruyama, and K. Sakata, “ $(\text{Bi}_{1/2}\text{Na}_{1/2})\text{TiO}_3$ – $\text{BaTiO}_3$  System for Lead-Free Piezoelectric Ceramics,” *Jpn. J. Appl. Phys.*, **30**, 2236–9 (1991).
- <sup>6</sup>B. Jaffe, W. R. Cook, and H. Jaffe, *Piezoelectric Ceramics*. Academic Press, London, 1971.
- <sup>7</sup>E. Sapper, S. Schaab, W. Jo, T. Granzow, and J. Rödel, “Influence of Electric Fields on the Depolarization Temperature of Mn-Doped  $(1-x)\text{Bi}_{1/2}\text{Na}_{1/2}\text{TiO}_3$ – $\text{BaTiO}_3$ ,” *J. Appl. Phys.*, **111**, 014105, 6pp (2012).
- <sup>8</sup>M. Cheng, H. Guo, S. P. Beckhman, and X. Tan, “Creation and Destruction of Morphotropic Phase Boundaries Through Electrical Poling: A Case Study of Lead-Free  $(\text{Bi}_{1/2}\text{Na}_{1/2})\text{TiO}_3$ – $\text{BaTiO}_3$  Piezoelectrics,” *Phys. Rev. Lett.*, **109**, 107602, 5pp (2012).
- <sup>9</sup>S. T. Zhang, A. B. Kouna, W. Jo, C. Jamin, K. Seifert, T. Granzow, J. Rödel, and D. Damjanovic, “High-Strain Lead-Free Antiferroelectric Electrostrictors,” *Adv. Mater.*, **21**, 4716–20 (2009).
- <sup>10</sup>M. Abazari, A. Safari, S. S. N. Bharadwaja, and T. McKinstry, “Dielectric and Piezoelectric Properties of Lead-Free  $(\text{Bi},\text{Na})\text{TiO}_3$ -Based Thin Films,” *S. Appl. Phys. Lett.*, **96**, 082903, 3pp (2010).
- <sup>11</sup>H. W. Cheng, X. J. Zhang, S. T. Zhang, Y. Feng, Y. F. Chen, and Z. G. Liu, “Combinatorial Studies of  $(1-x)\text{Na}_{0.5}\text{Bi}_{0.5}\text{TiO}_3$ – $\text{BaTiO}_3$  Thin-Film Chips,” *Appl. Phys. Lett.*, **85**, 2319–21 (2004).
- <sup>12</sup>N. Scarisoreanu, F. Craciun, V. Ion, S. Birjega, and M. Dinescu, “Structural and Electrical Characterization of Lead-Free Ferroelectric  $\text{Na}_{1/2}\text{Bi}_{1/2}\text{TiO}_3$ – $\text{BaTiO}_3$  Thin Films Obtained by PLD and RF-PLD,” *Appl. Surf. Sci.*, **254**, 1292–7 (2007).
- <sup>13</sup>Y. Guo, D. Akai, K. Sawada, and M. Ishida, “Dielectric and Ferroelectric Properties of Highly (100)-Oriented  $(\text{Na}_{0.5}\text{Bi}_{0.5})_{0.94}\text{Ba}_{0.06}\text{TiO}_3$  Thin Films Grown on  $\text{LaNiO}_3/\text{Al}_2\text{O}_3/\text{Si}$  Substrates by Chemical Solution Deposition,” *Solid State Sci.*, **10**, 928–33 (2008).
- <sup>14</sup>D. A. San José, R. Jiménez, I. Bretos, and M. L. Calzada, “Lead-Free Ferroelectric  $(\text{Na}_{1/2}\text{Bi}_{1/2})\text{TiO}_3$ – $\text{BaTiO}_3$  Thin Films in the Morphotropic Phase Boundary Composition: Solution Processing and Properties,” *J. Am. Ceram. Soc.*, **92**, 2218–25 (2009).
- <sup>15</sup>B. Wylie-Van Eerd, D. Damjanovic, N. Klein, N. Setter, and J. Trodahl, “Structural Complexity of  $(\text{Na}_{0.5}\text{Bi}_{0.5})\text{TiO}_3$ – $\text{BaTiO}_3$  as Revealed by Raman Spectroscopy,” *Phys. Rev. B*, **82**, 104112, 7pp (2010).
- <sup>16</sup>Y. Hiruma, Y. Watanabe, H. Nagata, and T. Takenaka, “Phase Transition Temperatures of Divalent and Trivalent Ions Substituted  $(\text{Bi}_{1/2}\text{Na}_{1/2})\text{TiO}_3$  Ceramics,” *Key Eng. Mater.*, **350**, 93–6 (2007).
- <sup>17</sup>F. Cordero, F. Craciun, F. Trequatrini, E. Mercadelli, and C. Glassi, “Phase Transitions and Phase Diagram of the Ferroelectric Perovskite  $(\text{Na}_{0.5}\text{Bi}_{0.5})_{1-x}\text{Ba}_x\text{TiO}_3$  by Anelastic and Dielectric Measurements,” *Phys. Rev. B*, **81**, 144124, 10pp (2010).
- <sup>18</sup>J. Yao, L. Yan, W. Ge, L. Luo, J. Li, and D. Viehland, “Evolution of Domain Structures in  $\text{Na}_{1/2}\text{Bi}_{1/2}\text{TiO}_3$  Single Crystals with  $\text{BaTiO}_3$ ,” *Phys. Rev. B*, **83**, 054107, 7pp (2011).
- <sup>19</sup>W. Jo, S. Silke, E. Sapper, L. A. Schmitt, H. J. Kleee, A. J. Bell, and J. Rödel, “On the Phase Identity and its Thermal Evolution of Lead Free  $(\text{Bi}_{1/2}\text{Na}_{1/2})\text{TiO}_3$ –6 mol%  $\text{BaTiO}_3$ ,” *J. Appl. Phys.*, **110**, 074106, 9pp (2011).
- <sup>20</sup>V. Dorcet, G. Troillard, and P. Boullay, “Reinvestigation of Phase Transitions in  $\text{Na}_{0.5}\text{Bi}_{0.5}\text{TiO}_3$  by TEM. Part I: First Order Rhombohedral to Orthorhombic Phase Transition,” *Chem. Mater.*, **20**, 5061–73 (2008).
- <sup>21</sup>A. A. Bokov and Z. G. Ye, “Recent Progress in Relaxor Ferroelectrics with Perovskite Structure,” *J. Mater. Sci.*, **41**, 31–52 (2006).
- <sup>22</sup>M. Alguero, H. Amorin, T. Hungria, J. Ricote, R. Jimenez, A. Castro, P. Ramos, J. Galy, J. Holc, and M. Kosec, “Nanostructured Ceramics of Perovskite Morphotropic Phase Boundary Materials,” *Adv. Multifunctional Mater. Syst.*, **216**, 3–18 (2010).
- <sup>23</sup>D. P. Mezcuca, R. Sirera, I. Bretos, L. F. Cobas, R. E. Galindo, D. Chateigner, J. Ricote, R. Jimenez, and M. L. Calzada, “Morphotropic Phase Boundary in Solution Derived  $(\text{Bi}_{0.5}\text{Na}_{0.5})_{1-x}\text{Ba}_x\text{TiO}_3$  Thin Films: Part I Crystalline Structure and Compositional Depth Profile,” *J. Am. Ceram. Soc.*, in press.
- <sup>24</sup>Y. Bai, G. P. Zheng, and S. Q. Shi, “Abnormal Electrocaloric Effect of  $\text{Na}_{0.5}\text{Bi}_{0.5}\text{TiO}_3$ – $\text{BaTiO}_3$  Lead Free Ferroelectric Ceramics Above Room Temperature,” *Mater. Resch. Bull.*, **46**, 1866–9 (2011).
- <sup>25</sup>X.c. Zheng, G. P. Zheng, Z. Lin, and Z. Y. Jiang, “Thermo-Electrical Energy Conversion in  $\text{Na}_{0.5}\text{Bi}_{0.5}\text{TiO}_3$ – $\text{BaTiO}_3$  Thin Films Prepared by Sol-Gel Method,” *Thin Solid Films*, **522**, 125–8 (2012).
- <sup>26</sup>A. S. Mischenko, Q. Zhang, J. F. Scott, R. W. Watmore, and N. D. Mathur, “Giant Electrocaloric Effect in Thin-Film  $\text{PbZr}_{0.95}\text{Ti}_{0.05}\text{O}_3$ ,” *Science*, **311**, 1270–1 (2006).
- <sup>27</sup>I. Bretos, D. A. San José, R. Jiménez, J. Ricote, and M. L. Calzada, “Evidence of Morphotropic Phase Boundary Displacement in Lead-Free  $(\text{Bi}_{0.5}\text{Na}_{0.5})_{1-x}\text{Ba}_x\text{TiO}_3$  Polycrystalline Thin Films,” *Mater. Lett.*, **65**, 2714–6 (2011).
- <sup>28</sup>J. R. Fernandes, F. A. de Sá, J. L. Santos, and E. Joanni, “Optical Fiber Interferometer for Measuring the  $d_{33}$  Coefficient of Piezoelectric Thin Films with Compensation of Substrate Bending,” *Rev. Sci. Instrum.*, **73**, 2073, 5pp (2002).
- <sup>29</sup>D. Rivero, L. Pardo, and R. Jiménez, “Instalación Para Medir el Lazo de Histéresis y las Corrientes de Conmutación en Láminas Delgadas de Materiales Ferroeléctricos,” *Rev. Cub. Física*, **126**, 169–73 (2009).
- <sup>30</sup>R. Jiménez, C. Alemany, M. L. Calzada, A. González, J. Ricote, and J. Mendiola, “Processing Effects on the Microstructure and Ferroelectric Properties of Strontium Bismuth Tantalate Thin Films,” *Appl. Phys. A*, **75**, 607–15 (2002).
- <sup>31</sup>User Manual Vision Software. Radiant Technologies Inc., Downloadable from <http://www.ferrodevices.com/>, 1999.
- <sup>32</sup>M. Alguero, J. Ricote, R. Jimenez, J. Carreaud, B. Dkhil, J. M. Kiat, J. Holc, and M. Kosec, “Size Effect in Morphotropic Phase Boundary  $\text{Pb}(\text{Mg}_{1/3}\text{Nb}_{2/3})\text{O}_3$ – $\text{PbTiO}_3$ ,” *Appl. Phys. Lett.*, **91**, 112905, 3pp (2007).
- <sup>33</sup>M. Alguero, M. Stewart, M. G. Cain, P. Ramos, J. Ricote, and M. L. Calzada, “Properties of Morphotropic Phase Boundary  $\text{Pb}(\text{Mg}_{1/3}\text{Nb}_{2/3})\text{O}_3$ – $\text{PbTiO}_3$  Films with Submicron Range Thickness on Si Based Substrates,” *J. Phys. D: Appl. Phys.*, **43**, 205401, 7pp (2010).
- <sup>34</sup>H. Hitham, R. Jiménez, J. Ricote, A. Alguero, and M. L. Calzada, “Improvement of the Remnant Polarization of  $0.65\text{Pb}(\text{Mg}_{1/3}\text{Nb}_{2/3})\text{O}_3$ – $0.35\text{PbTiO}_3$  Thin Films in a Multilayer Composite,” *Thin Solid Films*, **519**, 6467–71 (2011).
- <sup>35</sup>W. Jo, J. E. Daniels, J. L. Jones, X. Tan, P. A. Thomas, D. Damjanovic, and J. Rödel, “Evolving Morphotropic Phase Boundary in Lead-Free  $(\text{Bi}_{1/2}\text{Na}_{1/2})\text{TiO}_3$ – $\text{BaTiO}_3$  Piezoceramics,” *J. Appl. Phys.*, **109**, 014110, 7pp (2011).
- <sup>36</sup>I. Levin and M. I. Reaney, “Nano- and Mesoscale Structure of  $\text{Na}_{1/2}\text{Bi}_{1/2}\text{TiO}_3$ : A TEM Perspective,” *Adv. Funct. Mater.*, **22**, 3445–52 (2012).
- <sup>37</sup>W. Jo, J. Daniels, D. Damjanovic, W. Kleeman, and J. Rödel, “Two-Stage Processes of Electrically Induced-Ferroelectric to Relaxor Transition in  $0.94(\text{Bi}_{1/2}\text{Na}_{1/2})\text{TiO}_3$ – $0.06\text{BaTiO}_3$ ,” *Appl. Phys. Lett.*, **102**, 192903, 4pp (2013).
- <sup>38</sup>R. Jiménez and M. L. Calzada, “Behaviour of the Ferroelectric Polarization as a Function of Temperature in Sol-Gel Derived Strontium Bismuth Tantalate Thin Films,” *J. Sol-Gel. Sci. Technol.*, **42**, 277–86 (2007). □